Quantifying uncertainties in climate data: measurement limitations of naturally ventilated thermometer screens

Quantifying uncertainties in climate data: measurement limitations of naturally ventilated thermometer screens

Environmental Research Communications

OPEN ACCESS

RECEIVED
10 May 2021

REVISED
8 June 2021

ACCEPTED FOR PUBLICATION
21 June 2021

PUBLISHED
30 June 2021

LETTER

Quantifying uncertainties in climate data: measurement limitations of naturally ventilated thermometer screens

R Giles Harrison and Stephen D Burt

Department of Meteorology, University of Reading, Earley Gate, Reading, RG6 6ET United Kingdom

E-mail: r.g.harrison@reading.ac.uk

Keywords: climate data, air temperature, Stevenson screen, radiation error, thermometer time response

Supplementary material for this article is available online

Abstract

Climate science depends on accurate air temperature measurement. To achieve this, well ventilated thermometers protected from direct sunlight and precipitation are needed, commonly through using louvred enclosures known as screens or shields. Maintaining good natural ventilation is critical for accurate measurements. Ventilation effects on air temperature uncertainties are quantified here using an aspirated thermometer as a reference, for air temperatures spanning −2.8 °C to 35.5 °C. Of 81462 5 min mean temperature values obtained, 50% were within ±0.07 °C of the reference and only 2% lay beyond −0.66 °C to 0.47 °C, where negative values represent the naturally ventilated screen thermometer underestimating air temperature. Larger absolute differences arose from a combination of radiation exchange and time response effects, which are separated here. Firstly, using 20s data, the exponential time response of the naturally ventilated thermometer is shown to vary with wind speed u as $u^{-0.5}$, and exceeds the conventional 1 min averaging time for wind speeds up to 5 ms^{-1} (at 2 m height), increasing to at least 15 min when calm. Secondly, radiation exchange effects (both by day and by night) dominated at low wind speeds (<1 ms^{-1} at 2 m height). Insufficient time response damps recording of temperature extremes, potentially also influencing climatological means. A new method to reduce the uncertainties is presented. This reduces negative skew in the temperature bias from −1.05 to −0.26, and, for almost 90% of the data, also reduces the spread.

1. Introduction

Air temperature is a central parameter for climate studies. Nevertheless, it is troublesome to measure accurately, requiring standardised protective thermometer enclosures. These commonly operate by passing air naturally over the thermometers, whilst providing shelter from direct sunlight and rain. As measurements of 'air temperature' obtained with naturally ventilated thermometer screens form the backbone of the instrumental climate record, recognising the associated uncertainty in the temperature measurements obtained is important. Here, the limitations of natural ventilation on thermometers in a standard screen is investigated experimentally and quantified, with corrections proposed to improve the measurements.

In the UK and Ireland, successors of the thermometer enclosure (or 'screen') design originated by Thomas Stevenson and adopted by the British Meteorological Office from the 1870s are still widely used (Gaster 1882, Burt 2013). Operation of a Stevenson screen depends on natural airflow, but this is variable and occasionally insufficient for accurate air temperature measurement. This fundamental limitation was originally recognised by Aitken (1884), and has subsequently been confirmed by numerous national and international screen comparisons (see, for example, Harrison 2010, Lacombe *et al* 2011, Clark *et al* 2014 and Buisan *et al* 2015), with empirical and theoretical corrections investigated and proposed (e.g. Erell *et al* 2005, Nakamura and Mahrt, 2005, Bernard et al 2019). Naturally ventilated thermometer screens nevertheless remain in widespread use globally, with many derivative versions (Sparks 1972, Parker 1994), including changes in construction materials from wood to plastic (Perry *et al* 2007). These arrangements usually provide the daily climatological mean, maximum and minimum temperatures, as well as at other times, whether read manually by an observer or, increasingly, logged by computer.

Here, an experimental comparison is made between temperatures found from a 'traditional' naturally ventilated thermometer screen, with those obtained from an aspirated thermometer typical of modern climate measurement networks (Richardson *et al* 1999, Diamond *et al* 2013). Improved time resolution now available (e.g. compared with Nakamura and Mahrt (2005)) allows further quantification of the absolute air temperature accuracy of the traditional screen, separating lag time and radiation effects. Explicit parameterisation of the lag time variation with wind speed is provided, and a new method for temperature bias correction evaluated.

2. Air temperature measurement considerations

Two principal factors influence the accuracy of air temperatures measured using a naturally ventilated thermometer screen (NVTS): response time and radiation error (Brock and Richardson 2001, Harrison 2014). Firstly, the time response (as characterised by the exponential lag time) determines how quickly the NVTS thermometer responds to changes in air temperature. If the response time exceeds that of environmental air temperature fluctuation timescales, the resulting damped response will underestimate extreme values. The second factor, radiation error, arises from direct heating and cooling effects on the NVTS, from radiation exchange with its surroundings.

2.1. Response time

Power law relationships with wind speed are typically used to describe heat transfer, such as for the time response of a cylindrical thermometer sensor (Burt and dePodesta 2020). In the case of a thermometer in a naturally ventilated screen, the exponential lag time τ follows a power law equation of the form

$$\tau = Au^n \tag{1}$$

where u is the wind speed at screen height (HMSO 1981). n is typically -½, and A varies with the screen size and type (Harrison2011). Assuming $A = 8.2$ for a Stevenson screen with u in ms^{-1} (Bryant 1968), for $u = 1\ \mathrm{ms}^{-1}$ then $\tau = 8.2$ min. The lag time can be determined experimentally from observing temperature changes (e.g. Harrison 2014). If the environmental temperature rises steadily from T_a at a rate K, a thermometer of finite lag time τ will show a lagged temperature variation with time $T(t)$ given by

$$T(t) = -K\tau + Kt + T_a + e^{-t/\tau}[(T_0 - T_a) + K\tau] \tag{2}$$

where T_0 is the initial reading of the finite lag thermometer (HMSO 1981). τ can be found by using measurements from a second thermometer of negligible lag time (see also Supplementary Information (available online at stacks.iop.org/ERC/3/061005/mmedia)). The instantaneous temperature difference ΔT between two such thermometers a time t after a steady temperature change begins is

$$\Delta T = K\tau[e^{-\frac{t}{\tau}} - 1] + (T_0 - T_a)e^{-\frac{t}{\tau}} \tag{3}$$

2.2. Radiation exchange

The effect of solar heating on a thermometer-the 'radiation error'—can be represented as

$$\Delta T_R \propto Su^{-0.5} \tag{4}$$

where ΔT_R is the temperature difference between the thermometer and its environment, and S represents the short-wave radiation flux (Harrison 2014).

3. Experimental investigations

The inverse power law relationships of eq1 and eq4 show that the greatest influences on NVTS air temperature measurements occur in light winds. These have been investigated experimentally in a range of temperature, radiation and wind speed conditions, using instruments installed at the Reading University Atmospheric Observatory[1] (RUAO).

[1] The Observatory is described at: https://research.reading.ac.uk/meteorology/atmospheric-observatory/observatory-metadata/instruments-and-metadata/

3.1. Instrumentation

The experiments compared measurements from two accurate platinum resistance thermometers (PRTs), see e.g. Foken and Bange (2021), between 7 November 2019 and 16 August 2020. One PRT was exposed in a naturally ventilated screen, and the other, as a reference, in a force-ventilated screen alongside, drawing air at the same height. The NVTS was a MetSpec 'large' Stevenson screen, and the ventilated screen a Young model 43502. This screen was chosen for low power and therefore negligible heating, longevity and air intake from below to minimise wind direction effects. Both PRTs were the same make and model (Campbell Scientific PT100/3), for which the specified accuracy is better than ±0.1 °C at 0 °C, and within ±0.2 °C at ±100 °C (class AA in IEC (2008)); the Young screen specifies a maximum radiation error of 0.2 °C in 1000 Wm^{-2} radiation flux. Thermometer resistances were sampled every second by a Campbell Scientific CR9000X data logger. Many other meteorological instruments operate at the same site, including for measuring radiative fluxes and wind speed. In particular, the net radiation R_n is found using independent measurements of the downward and upwards 'long wave' and 'short wave' radiation fluxes, denoted by L_{dn}, L_{up}, S_g and S_{up} respectively, which are related by

$$R_n = (L_{dn} - L_{up}) + (S_g - S_{up}) \tag{5}$$

The four component Kipp and Zonen CNR4 radiometer used responds between 300nm to 2800nm for short wave radiation, and 4.5 to 42 μm for long wave radiation[2]. Wind speeds are also measured at a range of heights, using Vector Instruments A100 cup anemometers.

Differences in temperature between the naturally and mechanically ventilated thermometers are analysed for ventilation, lag time and radiation exchange effects. For this, the temperature difference, T_{diff}, is regarded as representing the NVTS temperature bias in determining the true air temperature, i.e. by assuming that the aspirated PRT provides air temperature with negligible uncertainty and time response.

3.2. Results

Examples of the combined meteorological measurements are provided in figure 1, for a clear day (25 December 2019) and a day of broken cloud (15 May 2020) respectively. The NVTS thermometer, conventionally referred to as the 'dry bulb' thermometer (T_{dry}) and the aspirated thermometer (T_{asp}) are shown in the upper panels, followed by the short wave and long wave radiative fluxes, wind speeds near the surface (at 1.12 m, 2 m and 5 m, denoted $u_{1.12}$, u_2 and u_5). The difference T_{diff} between T_{dry} and T_{asp}, defined as $T_{diff} = T_{dry} - T_{asp}$, is given in the lower panel, where positive T_{diff} indicates that the NVTS environment is warmer than air temperature as determined by the aspirated screen.

Figure 1 shows that T_{diff} is usually small ($\ll$0.5 °C) whenever the low-level wind exceeds about 1 ms^{-1}, but that larger values of T_{diff} occur at lesser wind speeds. For the December day (figure 1(a) to (d)), $T_{diff} > 1.0$ °C occurs in the late afternoon (figure 1(d)), when the wind speed drops, and T_{diff} becomes more variable: the effect is so pronounced that it can even be seen directly in figure 1(a), around the daily temperature maximum which is evidently over-estimated by the NVTS T_{dry}. For the May day (figure 1(e) to (h)), early and late parts of the day have relatively calm conditions, during which the largest T_{diff} occur. At about 06UTC, the post-sunrise rapid temperature increase highlights the slower response of the NVTS compared with the aspirated thermometer. Around noon, variable solar radiation (figure 1(f)) arises from broken cloud cover, yielding air temperature fluctuations. These fluctuations also illustrate the different time responses of the NVTS and aspirated sensors, as cloud-induced fluctuations initially appear in T_{diff}, but diminish after 12UTC, when the wind increases.

Figure 2(a) shows the range of the full temperature dataset, with figure 2(b) and table 1 summarising the distribution of T_{diff}. The preliminary conclusions from figure 1 are borne out, as very many values have $|T_{diff}| \ll 0.5$ °C, and 50% of T_{diff} values are within −0.07 °C to 0.06 °C. This also demonstrates that the two thermometers are closely matched. A skew towards negative T_{diff} indicates a tendency of the NVTS for air temperature underestimation.

4. Causes of the air temperature bias

Although table 1 shows that large $|T_{diff}|$ are rare, estimating or reducing air temperature biases becomes important when comparing temperatures predicted by weather forecast models with near-surface observations, and for assessing reliability of extreme values obtained at different sites.

4.1. Wind speed effects on temperature bias

Following the wind speed influence expected from section 2, T_{diff} is plotted against u_2, (figure 2(c)). This clearly demonstrates that the widest spread of T_{diff} occurs during low wind speeds, when $u_2 < 1 ms^{-1}$. The spread of

[2] At many sites, only the global solar irradiance S_g is measured, which dominates R_n during the day, e.g. at RUAO, $R_n \approx 1.3\, S_g + 63$, (for R_n and S_g in Wm^{-2}).

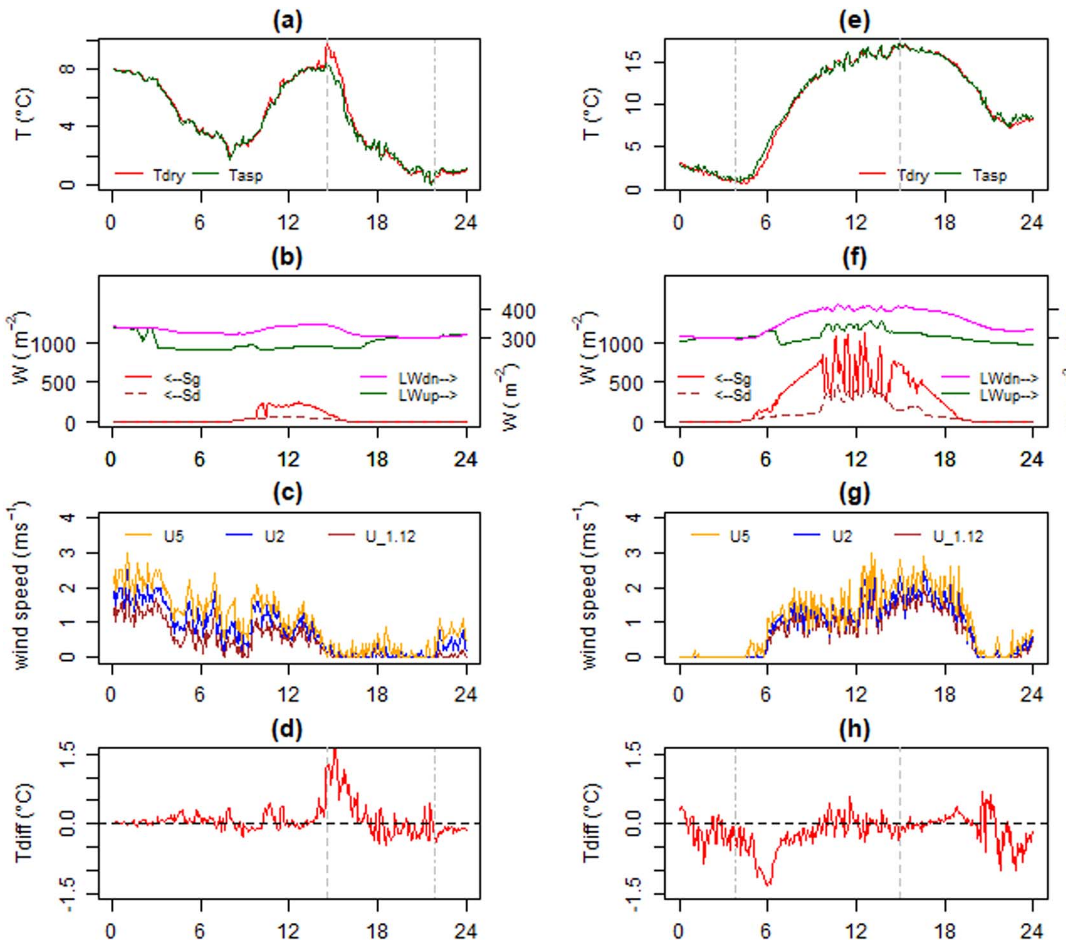

Figure 1. Time series (5 min averages of quantities plotted against hour of day UTC) from Reading University Atmospheric Observatory for, left-hand column, 25 December 2019 and, right-hand column, 15 May 2020. (a), (e) Stevenson screen air temperature (T_{dry}), aspirated thermometer temperature (T_{asp}). (b), (f) Radiative fluxes, global solar irradiance (S_g), diffuse solar irradiance (S_d), upwelling longwave (LW_{up}) and downwelling longwave (LW_{dn}). (c), (g) Wind speed, measured at 1.12 m ($u_{1.12}$), 2 m (u_2) and 5 m (u_5). (d), (h) Temperature difference T_{diff} between screen and aspirated thermometers, as $T_{diff} = T_{dry} - T_{asp}$. (Daily maximum and minimum temperatures are marked with dashed and dash-dotted lines respectively).

T_{diff} with u_2 can be represented by binning the T_{diff} values by wind speed and calculating the associated bin standard deviation. Figure 2(d) shows the form of the response. By fitting a power law, the variation in $|T_{diff}|$ can be found from $(1.96\,\sigma_{Tdiff}) = p\,u_2^q$, where $p = 0.311$ and $q = -0.36$. The exponent q is broadly consistent with the physical processes represented by equations (1) and (4).

4.2. Wind speed effects on screen time response

Because the lag time τ is a central parameter in the NVTS response, it is now determined explicitly. Assuming T_{asp} responds much more rapidly than the NVTS, successive samples of T_{asp} and T_{dry} during steady changes can provide relative rates of change to derive τ. (This methodology based on equation (2) is described in the Supplementary Information). Figure 3(a) shows the derived lag times, binned by wind speed. The τ variation with wind speed follows equation (1) with $A = (2.89 \pm 0.14)$ minutes and $n = -0.49 \pm 0.04$, where the uncertainties are 1.96 standard errors. τ becomes approximately steady for $u_2 > 2$ ms^{-1} (as for Harrison, 2011), but as $u_2 \to 0$, $\tau \to \infty$, although free convection will maintain a finite value in practice. Figure 3(b) provides additional context, using equation (3) to calculate the temperature error for different thermometer lag times, during a steady temperature increase. The temperature bias variation presented in figure 2(d) can therefore be largely explained by the increase of NVTS lag time with decreasing wind speed.

4.3. Representing the air temperature bias

Whilst the range of T_{diff} estimated in section 4.1 solely used wind speed information, further understanding of the physical processes may allow T_{diff} variations to be estimated from other quantities and therefore, potentially, corrected.

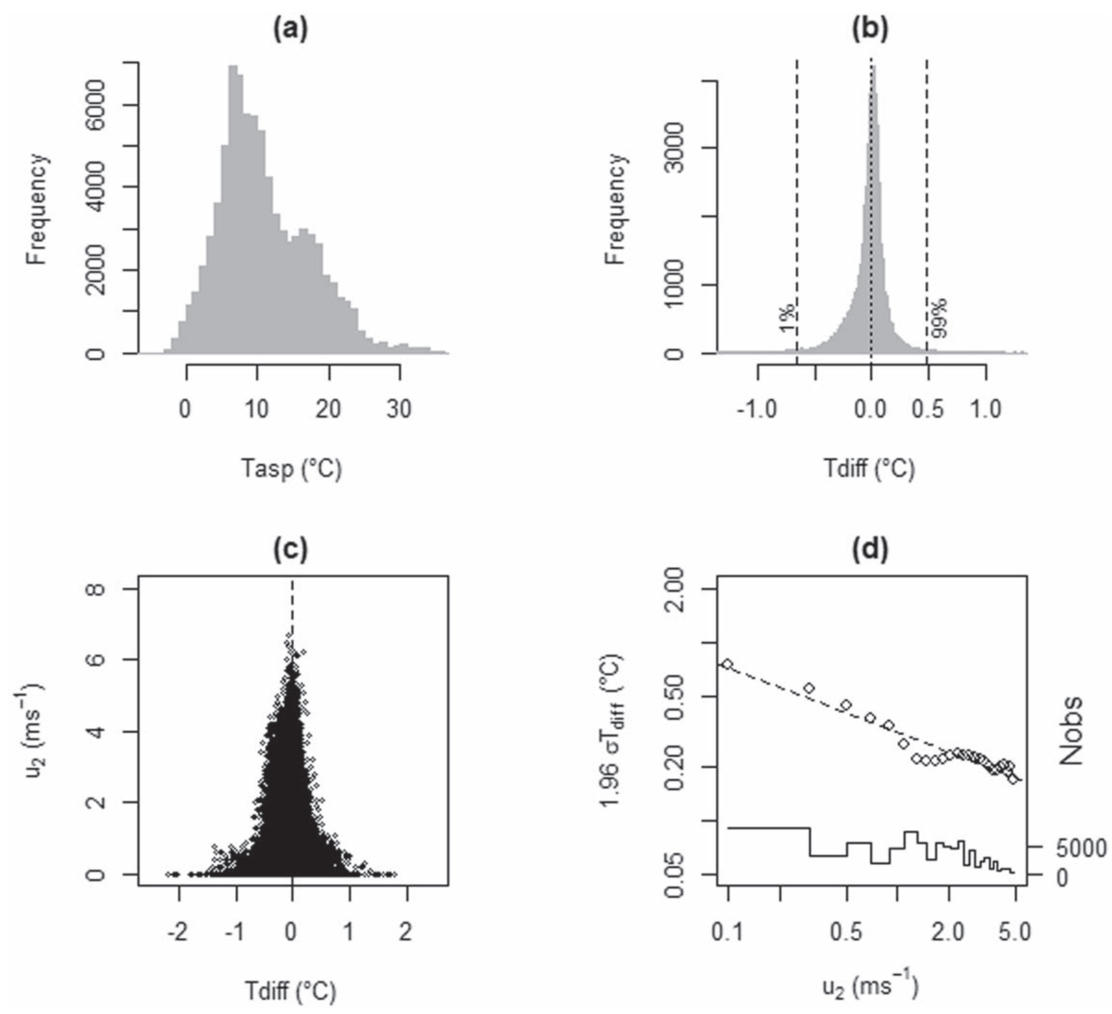

Figure 2. Distribution of (a) aspirated thermometer air temperatures (T_{asp}) made between 7 November 2019 and 16 August 2020 (5 min averages) at Reading, and (b) differences between naturally ventilated and aspirated thermometers ($T_{diff} = T_{dry} - T_{asp}$). (c) T_{diff} plotted against simultaneous u_2. (d) Spread of T_{diff} binned by wind speeds (in steps of 0.2 ms^{-1}) with a power law fit added and the number of observations (N_{obs}) in each bin shown. (5 min mean values are used and 1.96 standard deviations provide the 95% confidence range on T_{diff}).

The effect of time response on tracking rapid changes in air temperature is considered first, by assuming that the air temperature responds to the radiative heating or cooling of the surface beneath it. This assumption is justified by figure 4(a), which plots the rate of change of the more rapid aspirated thermometer, dT_{asp}/dt, against R_n. For most R_n values (-50 Wm^{-2} to 600 Wm^{-2}), there is proportionality between R_n and dT_{asp}/dt. The NVTS damping effect on rapid temperature changes will therefore also vary with R_n. This is made apparent in figure 4(b), by plotting T_{diff} against R_n. In this well-ventilated case ($u_2 > 1$ms^{-1}), T_{diff} varies inversely with R_n. This is consistent with the NVTS lag causing a negative temperature bias during rapid temperature increases, as suggested by figure 3(b).

Under light winds, only very slow NVTS changes occur in response to air temperature changes (figure 3(b)). The T_{diff} data have therefore been selected for light wind conditions. During poor ventilation ($u_2 < 0.5$ms^{-1}), figure 4(c) shows that the response of T_{diff} to R_n is reversed from figure 4(b), *i.e.* T_{diff} becomes directly proportional to R_n, consistent with the radiation error response of equation (4). For intermediate ventilation (0.5ms^{-1} $< u_2 <$ 1ms^{-1}), figure 4(d), T_{diff} remains proportional to R_n, but less strongly so.

To summarise, the two physical processes influencing the accuracy of air temperatures, as outlined in section 2, have been distinguished. At low wind speeds ($u_2 < 0.5$ ms^{-1}), direct radiation exchange dominates and T_{diff} is directly proportional to R_n. At greater wind speeds ($u_2 > 1$ ms^{-1}), T_{diff} becomes inversely proportional to R_n, indicating that the time response effects become dominant. In either case, a linear approximation satisfactorily represents the variation; table 2 lists the coefficients determined.

Table 1. Summary statistics of temperature differences.

Quantity	sample number	Min (°C)	Lowest percentile (°C)	Lower quartile (°C)	Median (°C)	Mean (°C)	Third quartile (°C)	Upper percentile (°C)	Max (°C)
T_{diff} (5 min means)	81462	−2.19	−0.66	−0.07	0.00	−0.022	0.06	0.47	1.75

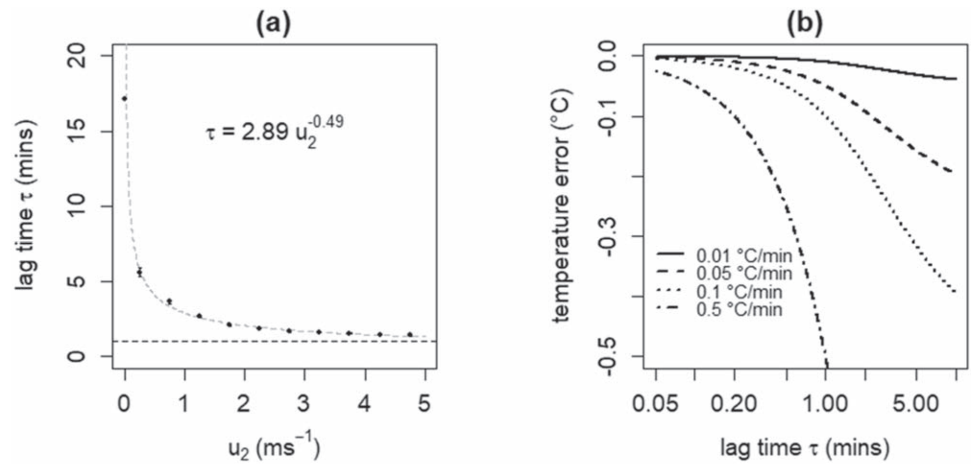

Figure 3. (a) Lag time τ calculated for the naturally ventilated screen by assuming a first order response, with a power law fit added (dashed line marks $\tau = 1$ min). Values are medians, using 20s data binned into wind speed steps of 0.5 ms^{-1}. (b) Calculated difference between air temperature and thermometer temperature after 5 min for different lag times, assuming a steady rate of temperature change.

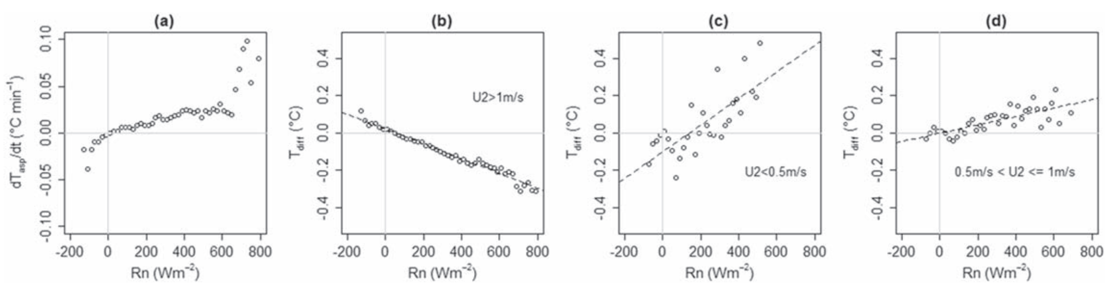

Figure 4. (a) Rate of change of aspirated temperature against binned (20 Wm^{-2} steps) net radiation R_n. (b), (c), (d) NVTS-aspirated temperature differences T_{diff}, binned and averaged into the same R_n steps, for (b) well ventilated conditions ($u_2 > 1$ ms^{-1}), (c) calm conditions ($u_2 < 0.5$ ms^{-1}) and (d) intermediate ventilated conditions (0.5 ms^{-1} $< u_2 \leqslant 1$ ms^{-1}). (Values used are 5 min means; bin averages removed for bins with fewer than 5 values. Unweighted least-squares linear fits have been added in (b), (c) and (d)).

Table 2. Coefficients of fitted lines to $T_{diff} = m\,R_n + c$.

Conditions	Gradient m (°C W^{-1}m^2)	Intercept c (°C)	Coefficient of determination R^2
Well ventilated $u_2 > 1$ ms^{-1}	-4.00×10^{-4}	0.023	0.98
Moderately ventilated 0.5 ms^{-1} $< u_2 \leqslant 1$ ms^{-1}	2.27×10^{-4}	-0.0015	0.58
Calm $u_2 \leqslant 0.5$ms^{-1}	7.17×10^{-4}	-0.101	0.57

4.4. Correcting the air temperature bias

These findings are now applied to the entire dataset. In figure 5(a), dT_{asp}/dt is shown, plotted against simultaneous measurements of R_n and u_2. Regions of rapid temperature changes appear on figure 5(a) for the greatest and least R_n values, as expected from figure 4(a). These are absent for $u_2 < 1$ms^{-1}, and the proportionality with R_n emphasises the radiation effects in this region. (This also justifies the different fitted lines of figures 4(b), (c) and (d)).

In figure 5(b), all T_{diff} values obtained are plotted against R_n and u_2 and characteristic regimes are again apparent. Firstly, when the wind speed u_2 exceeds about 1ms^{-1}, with large R_n (e.g. strong sunshine), the NVTS temperature falls below air temperature (blue on the right of figure 5(b)), whereas, for negative R_n (e.g. a clear night), the NVTS temperature exceeds air temperature (red on the left of figure 5(b)). This arises because the NVTS response time is insufficient to cool or warm rapidly enough to track the air temperature change. Secondly, when u_2 is small ($<$1ms^{-1}), the NVTS temperature excess appears approximately proportional to R_n (increasingly red from left to right along the bottom of figure 5(b)). When calm and sunny, the NVTS radiation exchange is therefore dominated by solar heating. Together, these results confirm that, firstly, that the NVTS is

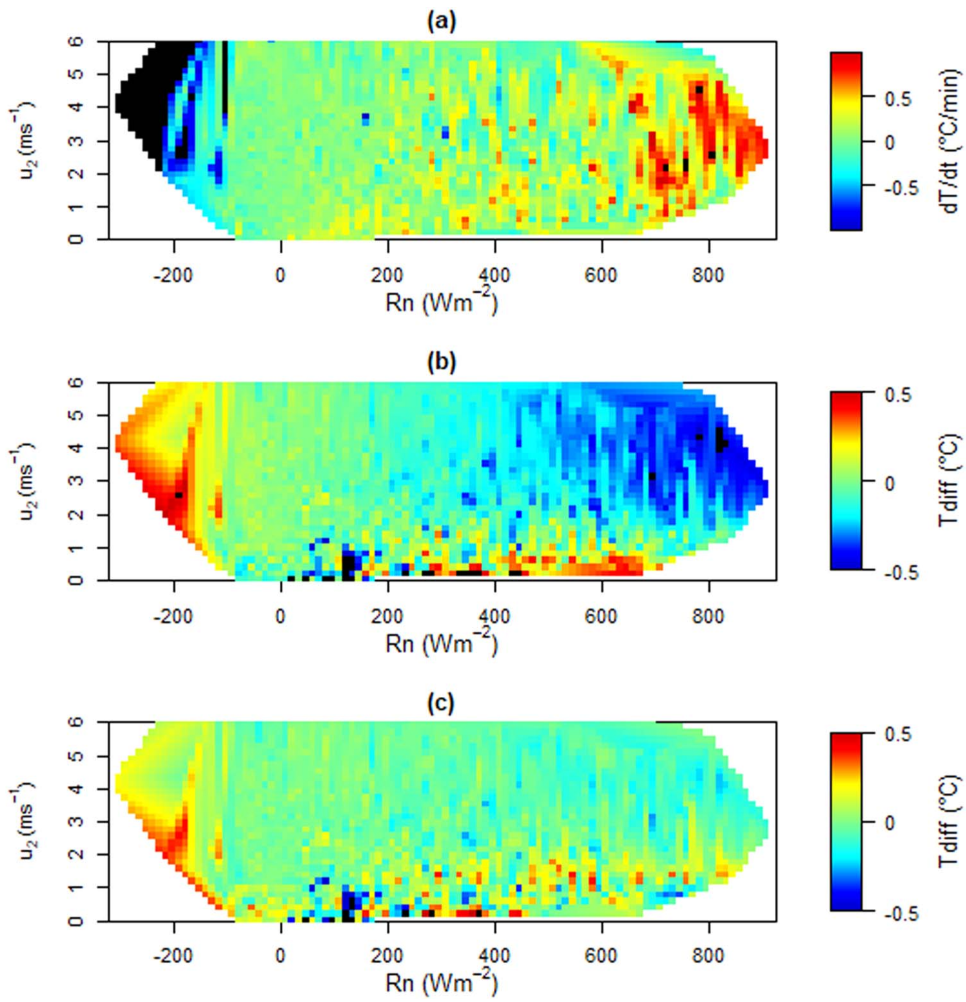

Figure 5. (a) Rate of change of temperature (aspirated thermometer), plotted against net radiation (R_n) and 2m windspeed u_2. (b) and (c) Temperature differences T_{diff} plotted against R_n and u_2, (b) uncorrected for naturally ventilated screen time response and radiation error and (c) corrected using the relationships in figure 4. (Values used are 5 min means. Black pixels mark values lying outside the range of the colour bar).

Table 3. Summary statistics for correction of air temperature uncertainties.

Ventilation conditions	Number of points	Proportion of values	Median (°C)		IQR (°C)	
			uncorrected	corrected	uncorrected	corrected
Calm $u_2 \leqslant 0.5\text{ms}^{-1}$	14939	18.3%	−0.07	0.05	0.320	0.317
Moderately ventilated $0.5\ \text{ms}^{-1} < u_2 \leqslant 1\ \text{ms}^{-1}$	10792	13.2%	0.0008	−0.004	0.140	0.141
Well ventilated $u_2 > 1\ \text{ms}^{-1}$	55731	68.4%	−0.01	0.001	0.110	0.079
All conditions	81462	100.0%	−0.02	0.009	0.13	0.11

unable to fully capture positive- or negative-going temperature fluctuations even when conditions are apparently well ventilated, and, secondly, during poorly ventilated conditions, that the NVTS temperature is strongly influenced by radiation exchange.

Use of the table 2 parameterisations as potential bias corrections to the data of figure 5(b) for different wind speed ranges is evaluated in figure 5(c). This demonstrates that the corrections act to diminish the screen temperature over-reading (red) and under-reading (blue) regions on the left and right-hand sides of figure 5(b), mitigating the time response effect. Further, the low wind speed radiation effects, apparent along the bottom of figure 5(b), are also reduced in figure 5(c). Table 3 summarises the T_{diff} properties with and without the adjustments applied. Overall, these adjustments lead to less spread in 87% of the T_{diff} data, and the negative skewness associated with the naturally ventilated screen's underestimation of air temperatures is reduced from −1.05 to −0.26.

5. Conclusions

Naturally ventilated thermometer screens permit accurate air temperature measurements, to ±0.1 °C in most circumstances. However, air temperature and the NVTS temperature can occasionally differ substantially by more than 0.5 °C in light winds because of a slow response. Absolute rates of temperature changes >0.5 °C min^{-1} occur in about 2% of cases in the mid-latitude UK (Burt and dePodesta 2020), but the variable response time of the NVTS limits its ability to track rapid temperature changes. The 1 min averaging period conventionally used in meteorology may therefore be insufficient with a NVTS. The coefficients explicitly determined here for the lag time parameterisation (equation 1), $A = 2.89$ min and $n = -0.49$, are useful for modelling screen time response, and establishing when the 1 min averaging criterion can be fulfilled.

The measured NVTS temperature is therefore only ever an approximation to air temperature. Likely temperature uncertainties can be estimated from the local wind speed, using measured or modelled values. Retrospective re-evaluation is possible: qualitative wind speed estimates using the Beaufort scale (e.g. Burt 2012) suggest, from figure 2(d), that when a wind strength of Beaufort force 3 (i.e. >4 ms^{-1}) can be established, the maximum air temperature uncertainty will be about 0.2 °C. Whilst the detailed corrections will depend on the situation, instruments and the sampling interval used, the methodology presented here uses physical principles which should generalise to similar NVTS operating in a standard manner.

Widespread and enduring use of naturally ventilated thermometer screens has yielded a long series of reliable measurements on which the instrumental climate record depends. However, even during appreciable wind speeds (3 to 5 ms^{-1} at 2m height), these results show that the time response of a large screen is never sufficient for rapid atmospheric changes to be fully captured. Consequently, until this effect of natural variability is removed by the more extensive use of aspirated thermometers throughout climate observation networks, an influence on some recorded extremes in the climate record cannot be ruled out. The findings here suggest that this will also apply to underestimation of maximum temperatures and overestimation of minimum temperatures during low wind conditions, which may also influence climatological mean values at such times.

Acknowledgments

We thank those concerned with maintaining the Observatory measurements throughout the COVID Pandemic, especially the University technical staff.

Data availability statement

The data that support the findings of this study are openly available at the following URL/DOI:http://doi.org/10.17864/1947.303.

ORCID iDs

R Giles Harrison https://orcid.org/0000-0003-0693-347X
Stephen D Burt https://orcid.org/0000-0002-5125-6546

References

Aitken J 1884 Thermometer screens *Proc Roy Soc Edin* **12** 661–96

Bernard J, Kéravec P, Morille B, Bocher E, Musy M and Calmet I 2019 Outdoor air temperature measurement: a semi-empirical model to characterize shelter performance *Climate* **7** 26

Brock F V and Richardson S J 2001 *Meteorological Measurement Systems.* (New York: Oxford University Press) p 290

Bryant D 1968 An investigation into the response of thermometer screens—the effect of wind speed on the lag time *Meteorol. Mag.* **97** 256

Buisan S T, Azorin-Molina C and Jimenez Y 2015 Impact of two different sized Stevenson screens on air temperature measurements *Int. J. Climatol.* **35** 4408–16

Burt S 2012 *The Weather Observer's Handbook* (Cambridge: Cambridge University Press) (https://doi.org/10.1017/CBO9781139152167)

Burt S 2013 An unsung hero in meteorology: Charles Higman Griffith (1830–1896) *Weather* **68** 135–8

Burt S and dePodesta M 2020 Response times of meteorological air temperature sensors *QJR Meteorol Soc* **146** 2789

Clark M R, Lee D S and Legg T P 2014 A comparison of screen temperature as measured by two Met Office observing systems *Int. J. Climatol.* **34** 2269–77

Diamond H J *et al* 2013 U.S. Climate Reference Network after one decade of operations: status and assessment *Bull. Amer. Meteorol. Soc.* **94** 485–98

Erell E, Leal V and Maldonado E 2005 Measurement of air temperature in the presence of a large radiant flux: an assessment of passively ventilated thermometer screens *Boundary-Layer Meteorol.* **114** 205–31

Foken T and Bange J 2021 Temperature sensors *Handbook of Atmospheric Measurements.* ed T Foken (Switzerland: Springer Nature) 185-210

Gaster F 1882 Report on experiments made at Strathfield Turgiss in 1869 with stands or screens of various patterns, devised and employed for the exposing of thermometers, in order to determine the temperature of the air. *Meteorological Office Quarterly Weather Report, Addendum for* 1879 [dated May 1880, published 1882]

Harrison R G 2010 Natural ventilation effects on temperatures within Stevenson screens *QJR Meteorol Soc* **136** 253–9

Harrison R G 2011 Lag-time effects on a naturally ventilated large thermometer screen *QJR Meteorol Soc* **137** 402–8

Harrison R G 2014 *Meteorological measurements and Instrumentation* (Chichester: Wiley) (https://doi.org/10.1002/9781118745793)

HMSO 1981 *Handbook of Meteorological Instruments: Measurement of Temperature* Meteorological Office2nd edn 2 (Her Majesty's Stationery Office)

IEC 2008 *Industrial platinum resistance thermometer* Edition 2.0 (International Electrotechnical Commission Geneva) IEC 60751 41

Lacombe M *et al* 2011 Instruments and observing methods report no. 106: WMO field intercomparison of thermometer screens/shields and humidity measuring instruments, Ghardaïa, Algeria, November 2008—October 2009 *Instruments and Observing Methods Report No. 106, WMO/TD-No. 1579* (Geneva, Switzerland)

Nakamura R and Mahrt L 2005 Air temperature measurement errors in naturally ventilated radiation screens *J Atmos Ocean Tech* **72** 1046–58

Parker D E 1994 Effects of changing exposure of thermometers at land stations *Int. J. Climatol.* **14** 1–31

Perry M C, Prior M J and Parker D E 2007 An assessment of the suitability of a plastic thermometer screen for climatic data collection *Int. J. Climatol.* **27** 267–76

Richardson S J, Brock F V, Semmer S R and Jirak C 1999 Minimizing errors associated with multiplate radiation shields *J Atm Oceanic Techn.* **16** 1862–72

Sparks W R 1972 *The Effect of Thermometer Screen Design on the Observed Temperature.* (Geneva: World Meteorological Organization) Publication No. 315, Available online at (https://library.wmo.int/doc_num.php?explnum_id=8131)